Designing a converging-beam electron gun and focusing solenoid

Stanley Humphries, Ph.D.

Field Precision LLC
E mail: techinfo@fieldp.com
Internet: https://www.fieldp.com

1 Goals and initial analysis

A frequent electron gun design goal is to produce a converging beam that matches to a focusing solenoid. This tutorial describes a case study for a system to generate a narrow electron beam at high current density and to transport it over a distance exceeding 8.0 cm for experiments on high-frequency microwave generation. I was given the following design goals:

Beam energy: $T_e = 120$ keV.

Beam current: $I = 2.0$ A.

Beam radius in solenoid: $r_w = 0.025$ cm.

Cathode radius: $r_c = 0.51$ cm.

Cathode temperature: 1000 °C.

Range of focusing magnetic field: $B_0 = 0.24 - 0.48$ tesla

Electric field on focusing electrode: < 100 kV/cm

Inner radius of focusing solenoid: 2.22 cm

To begin, I checked that it is theoretically possible to focus a beam with the given parameters to a waist with radius r_w (compression factor $\chi = r_c/r_w = 20$). (Note that all references in this report are to my book **Charged Particle Beams**, available for download on our Internet site at `http://www.fieldp.com/cpb.htm`.) Section 5.4 gives the distance L for a beam to expand radially from a waist by a factor of χ:

$$L = \frac{r_w F(\chi)}{\sqrt{2K}}, \tag{1}$$

where K is the generalized perveance and the function $F(\chi)$ is tabulated in the book. Inserting the parameters $r_w = 0.025$ cm, $F(20) = 14.86$ and $K = 6.158 \times 10^{-4}$, we find that $L \leq 10.6$ cm. The envelope angle at L is:

$$r' = \sqrt{2K}\ \sqrt{\ln(\chi)} \tag{2}$$

Inserting numerical values, we find that $r' = 0.0607$ radian. The value implies an approximate radius of curvature for the cathode of

$$R_c \leq \frac{r_c}{r'} = 8.4 \text{ cm}. \tag{3}$$

The radius of curvature in the final gun design is smaller because of two factors: 1) the negative lens effect at the aperture and 2) the need to compensate the beam divergence.

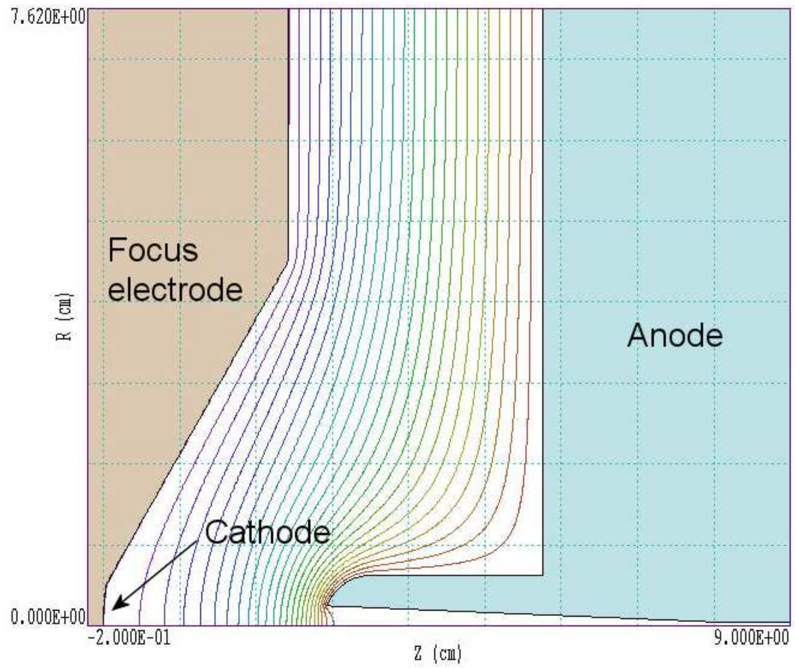

Figure 1: Initial electron gun design, z-r plot with equipotential lines and model electron orbits.

I used the design procedure described in Sect. 7.2 of **Charged Particle Beams** with the following constraints:

1. The cathode surface had radius of curvature centered at $z = R_c$.
2. The focusing electrode was inclined with respect to the outer edge of the cathode at the Pierce angle of 22.5^o.
3. The forward anode surface followed a spherical section centered at $z = R_c$ that intersected the axis at $z = R_a$.
4. The anode aperture had radius 0.25 cm.

2 Electron gun design

I generated an series of solutions to find a baseline gun geometry consistent with the goals. These runs were performed with zero divergence at the cathode, an ideal physical connection to the focusing electrode and no transport magnetic field. I varied R_c and R_a and also tuned-up other features of the simulation as the runs progressed. Table 1 shows the series of runs to coverge

Table 1: Initial gun design, parameter-space search.

r_c (cm)	Anode position (cm)	Current (A)	Divergence (degrees)
8.0	5.0	1.326	0.0
6.5	4.0	1.872	0.0
6.0	3.75	2.085	0.0
5.5	3.75	1.980	0.0
5.0	3.50	2.281	0.0
4.5	3.625	1.556	0.0
4.0	3.50	1.346	0.0
3.75	3.00	1.928	0.0
3.75	3.00	1.928	4.0
3.50	2.875	1.930	4.0

on the final geometry shown in Fig. 1. I added effects of cathode temperature when I was close to the desired solution. The cathode temperature was about 0.1 eV and the emission surface potential was 22 eV. The angular divergence at the emission surface was therefore 0.071 radians (4.0 deg). Figure 2 shows equipotentials and model particle orbits for the working geometry without and with divergence. Note the effect of field curvature at the extraction aperture. The root-mean-squared wait radius at 7.75 cm from the cathode surface was 0.018 cm.

To conclude the gun design, I added a gap between the cathode edge and focusing electrode consistent with manufacturing tolerances. Figure 2 shows a detail of the mesh near the cathode edge. In the initial run, the marked point was at same axial location as the cathode edge. In this case, the gap caused enhanced current and defocusing at the edge. I moved the point forward until the total current and beam envelope was the same as the ideal solution. I then put a radius on the sharp edge at the anode aperture for an estimate of the peak electric field on the anode. Figure 4 shows that $|\mathbf{E}|$ on the anode was less than 250 kV/cm. The maximum field stress on the negative electrodes was in the range 50-60 kV/cm.

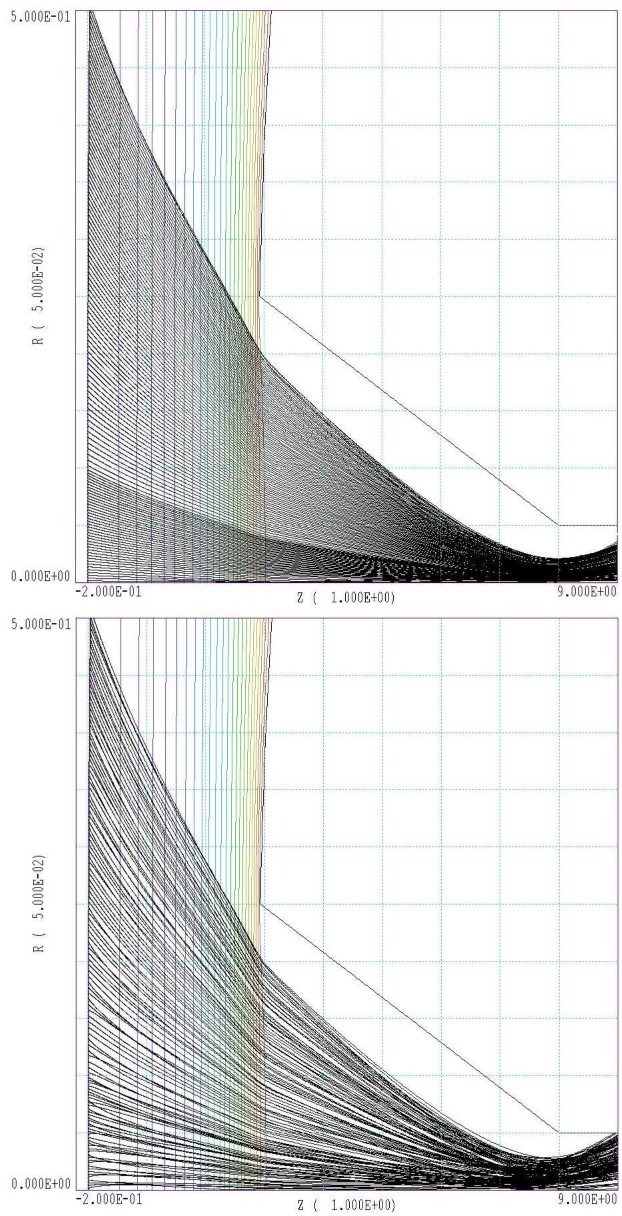

Figure 2: Equipotential lines and beam profiles for the solution of Fig. 1 with a strong radial magnification. Top: No beam divergence. Bottom: 4.0°divergence at the emission surface.

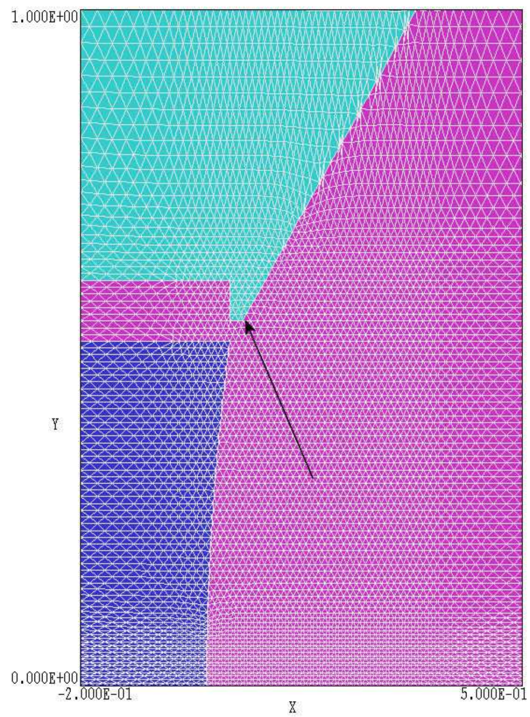

Figure 3: Detail of the mesh showing the gap between the cathode and focusing electrode.

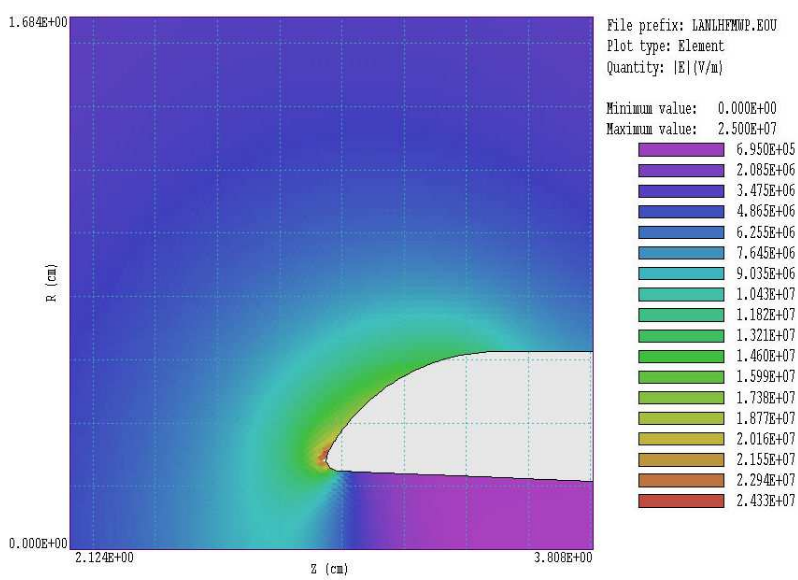

Figure 4: Plot of $|\mathbf{E}|$ near the tip of the anode extension.

3 Focusing solenoid

The minimum inner radius of the focusing solenoid coil was 2.22 cm (0.32 cm thick mandrel over a vacuum tube of radius 1.90 cm). The beam pulselength in the low duty cycle system was a few μs. Therefore, I considered a pulsed magnet coil to minimize size and complexity. An iron shield is essential to ensure that field level is small at the cathode and that field transition at the beam waist has a short axial length. The coil pulselength must be long enough to guarantee a uniform field distribution in the iron so that the field profile is close to the code prediction. The time Δt for a pulsed magnetic field to penetrate to a depth δ into a non-laminated iron shield is given approximately by:

$$\Delta t \cong \frac{\delta^2 \mu_0 \mu_r}{2\rho}. \quad (4)$$

In the equation μ_r is the relative magnetic permeability of the iron and ρ is the volume resistivity. In 1018 steel, the parameters are $\mu_r \cong 1000$ and $\rho = 1.01 \times 10^{-7}$ Ω-m. For a shield thickness $\delta = 0.0075$ m, Eq. 4 predicts that $\Delta t \cong 0.35$ s. To be conservative, I assumes a 2.5 s pulselength in the following calculations.

Figure 5 shows the dimensions of the solenoid determined from an extnded set of calculations. In the reference frame of the r-z plot, the upstream face of the coil is at position $z = 0$. The coil length of 15.24 cm (6.00") gives a flat field region ($\pm$0.5 %) about 10.0 cm (3.94") in length. The coil inner radius is $R_i = 2.22$ cm and outer radius is $R_o = 4.22$ cm. The magnetic shield has thickness 0.75 cm. The large shield opening on the downstream end allows insertion of microwave experiments. The shield has a small opning on the upstream side (0.3 cm radius) to ensure 1) isolation of cathode, 2) a sharp transition at the beam waist, and downstream field uniformity.

With a drive current of 38,000 A-turn, the solenoid produces a field $B_0 =$ 0.312 tesla. The blue curve in Fig. 6 shows the axial variation of on-axis field, $B_z(0, z)$. Note the broad-scale field variation at the open downstream end. The field profile would be the same at the upstream end without the radial shield extension. Such a profile Would give significant field at the cathode and poor beam convergence. Figure 7 shows the variation of $|\mathbf{B}|$ near the upstream end of the coil. Field values are well below saturation over the volume of the shield, confirming that the 0.75 cm thickness is sufficient.

We assume that coil is wound with #16 enameled copper magnet wire. Wire of this gauge is easy to wind, ensures a large number of turns for field uniformity, and has a moderate resistance. The corresponding drive voltage is well within capacity of the insulating enamel. The following Internet site gives useful data for magnet wire:

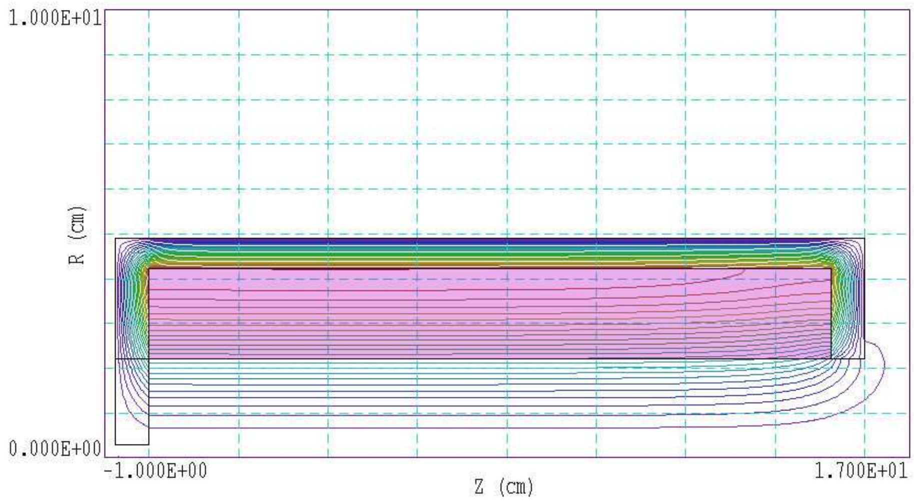

Figure 5: Transport solenoid assembly with coil highlighted. Horizontal grid spacing: 2.0 cm. Vertical grid spacing: 1.0 cm.

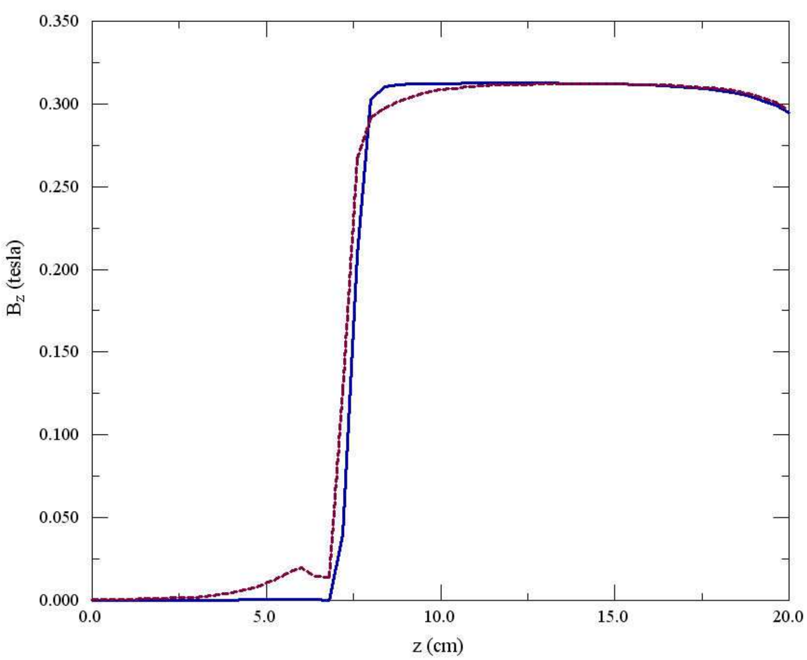

Figure 6: Variation of on-axis magnetic field, $B_z(0, z)$. The surface of the cathode is at position $z = 0.0$. Solid blue curve: baseline design. Dashed red curve: gap of width 0.16 cm in radial shield extension.

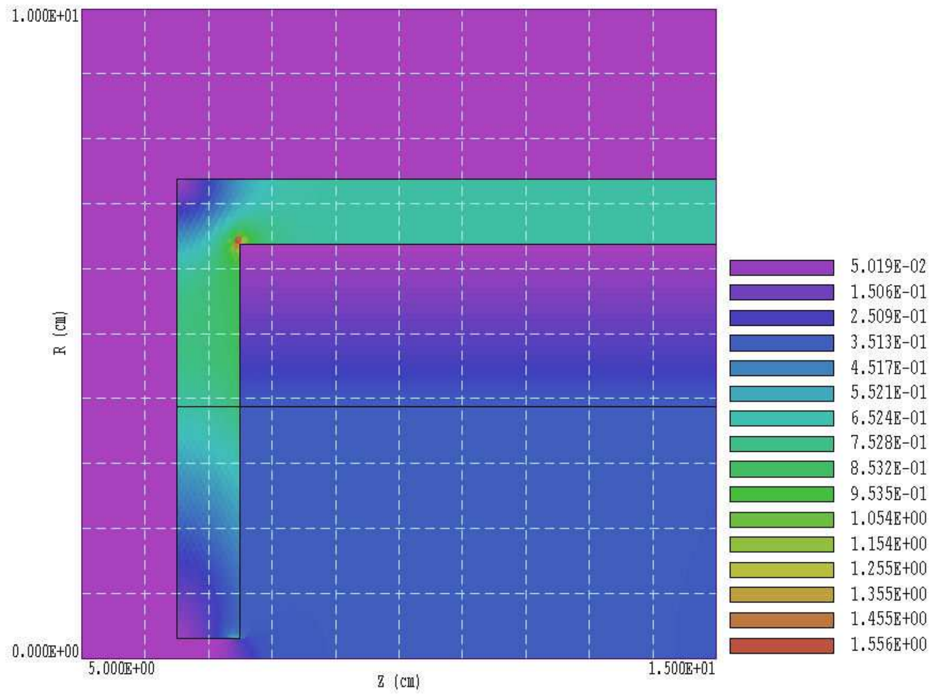

Figure 7: Spatial variation of $|\mathbf{B}|$ near the solenoid entrance, values in tesla.

`http://www.reawire.com/ind_dims_choose.asp`

The nominal diameter of bare #16 wire is 0.0508". A typical diameter with insulation is 0.0524". The wire resistance is 4.018 Ω/1000 ft. For the baseline coil dimensions, there are approximately 114 turns in each of 15 radial layers. The total number of turns is $N = 1710$. The drive current to achieve 38,000 A-turns is $I = 22.2$ A. The total wire length in the coil is given by:

$$L \cong 2\pi \frac{R_i + R_o}{2} N. \tag{5}$$

Inserting coil dimensions, we find $L = 346$ m or 1135 ft. The total coil resistance is $R = 4.56\Omega$. The drive voltage is $V = 101.2$ V and the resistive power dissipation is 2248 W. The total input energy during a 2.5 s pulse is $U = 5620.0$ J.

The bare wire radius of 0.0645 cm corresponds to a cross-section area of 1.308×10^{-2} cm^2. Taking a length $L = 3.46 \times 10^4$ cm, the volume of copper in the coil is 452.0 cm^3. With density 8.96 gm/cm^3, the mass of copper in the coil is $M = 4054.0$ gm. Copper has a specific heat $C_p = 0.38$ J/gm-^{o}C. The expected temperature rise in the wire is

$$\Delta T \cong \frac{U}{C_p M}. \tag{6}$$

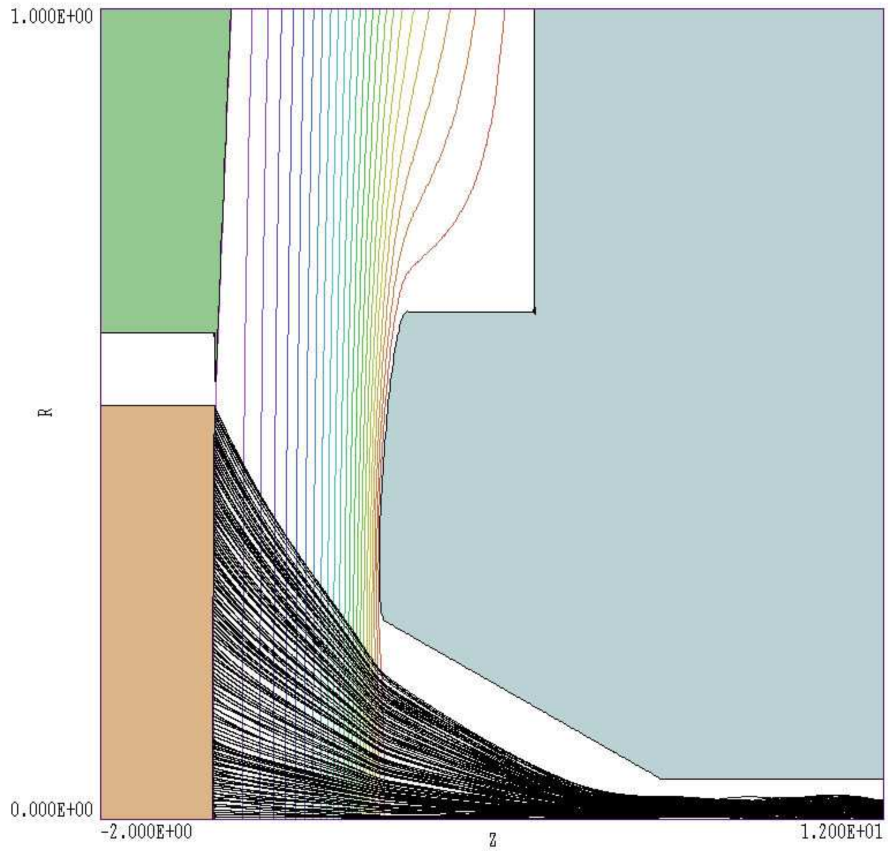

Figure 8: Self-consistent Trak solution for beam motion in the gun, matching region and transport solution. Plot shows model particle orbits and equipotential lines with a 14:1 radial magnification.

Inserting coil values in Eq. 6, we find a relatively small temperature difference $\Delta T = 3.7$ °C (6.5 °F).

4 Beam matching calculations

Figure 8 shows a complete self-consistent solution combining the gun described in Report 1 with the new solenoid. Note that there is a strong radial magnification – the radial extent of the plot is 1.0 cm and the axial length is 14.0 cm. The total drive current is 38,000 A-turn and the coil has been displaced +7.5 cm along the axis. This means that the upstream face of the iron shield is 6.75 cm from the cathode surface and the coil starts at z = 7.50 cm. Figure 9 is a true scale representation of the complete system with a superposition of gun electrodes and the solenoid assembly.

To conclude, I checked the effects of two variations in the system. The

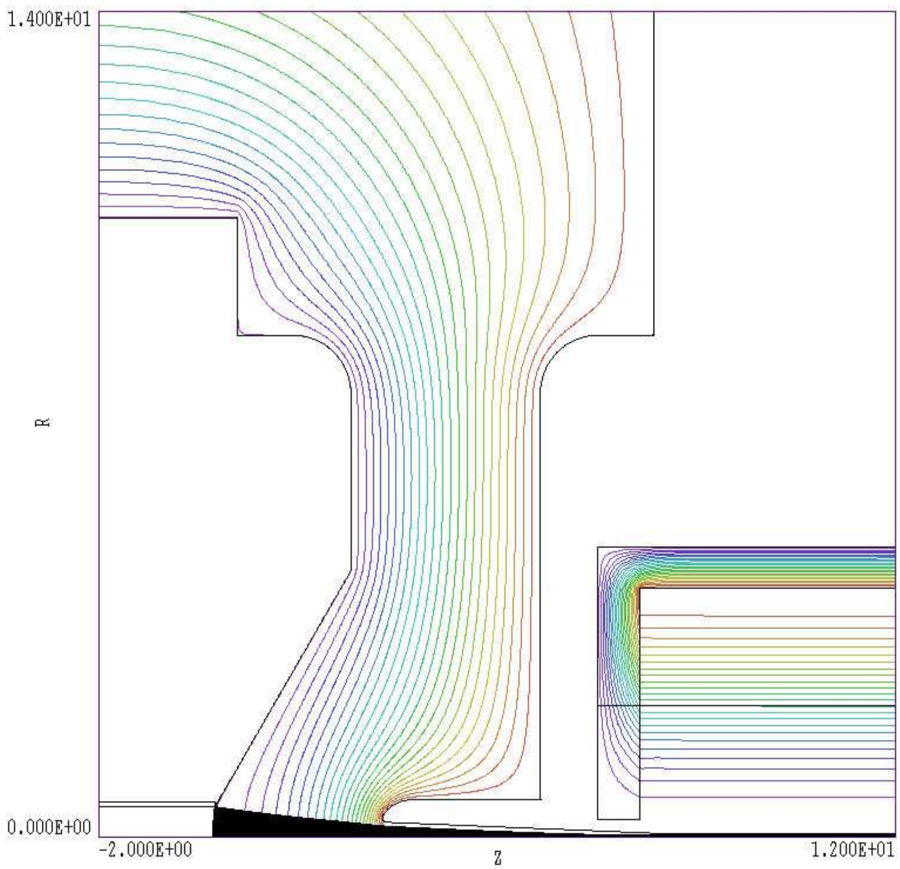

Figure 9: True-scale representation of the system showing the gun electrodes and components of the solenoid assembly.

first was the possibility of fabricating the upstream radial extension of the magnetic shield as a separate piece inside the vacuum tube. This arrangement leaves a gap of 1/16" (0.16 cm) in the magnet circuit (the thickness of the vacuum chamber wall). The dashed red line in Fig. 6 shows the resulting on-axis field variation. Some flux has been forced upstream and field uniformity near the transition has been degraded. Nonetheless, there was little effect on the beam solution. Therefore, the geometry remains as an option if it simplifies design of the system.

Finally, Figure 10 shows the effect of axial displacements of the solenoid assembly. A position error of 0.5 cm results in mismatching with large oscillations of the beam envelope. The position of the solenoid should be accutate to better than ± 1.0 mm. After analysis of series of runs with displacements from 7.0 to 8.0 cm in 0.25 cm steps, I expect that the ideal solenoid displacement is close to 7.375 cm. At this setting, the distance from the cathode surface to the upstream face of magnetic shield is 6.625 cm.

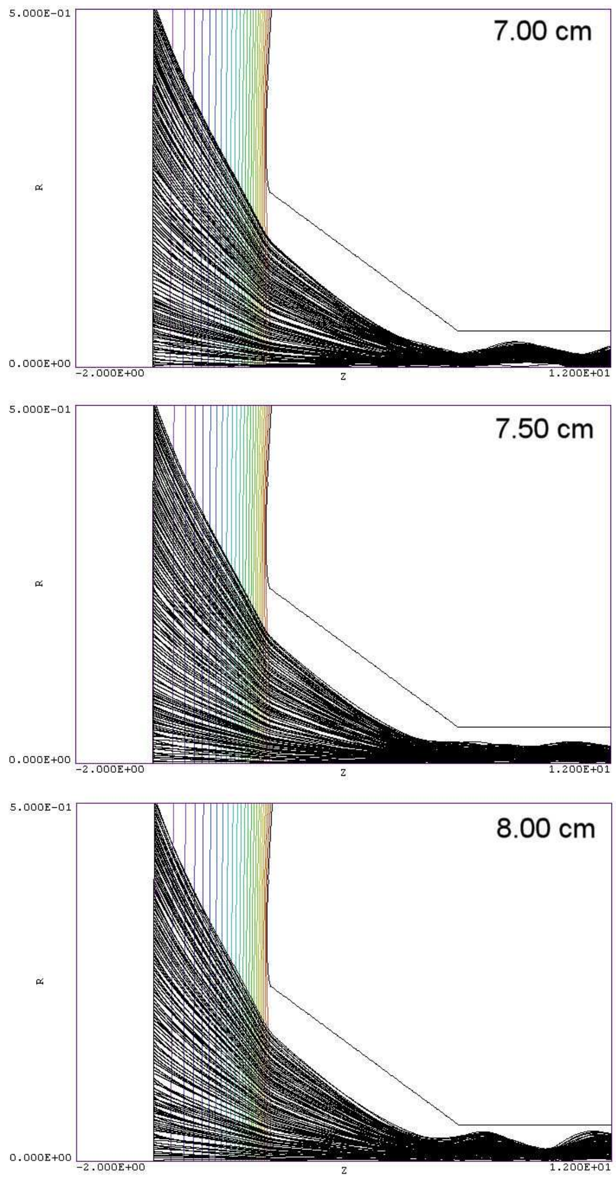

Figure 10: Beam envelope variations with changes in axial solenoid position. Distance from cathode surface to coil. Top: 7.0 cm. Middle: 7.5 cm. Bottom: 8.0 cm.